Received: 30 July 2021 | Revised: 28 April 2022 | Accepted: 28 June 2022 | Published on: 31 July 2022

DOI: 10.1002/joc.7800

RESEARCH ARTICLE

International Journal of Climatology RMetS

Thunderstorm days over Argentina: Integration between human observations of thunder and the world wide lightning location network lightning data

Fiorela Bertone[1] | **Gabriela Nicora**[2] | **Luciano Vidal**[3]

[1]Dirección de Servicios Sectoriales, Servicio Meteorologico Nacional, Buenos Aires, Argentina

[2]DEILAP, CITEDEF, Buenos Aires, Argentina

[3]Dirección de Productos de Modelación Ambiental y de Sensores Remotos, Servicio Meteorológico Nacional, Buenos Aires, Argentina

Correspondence
Fiorela Bertone, Dirección de Servicios Sectoriales, Servicio Meteorologico Nacional, Buenos Aires, Argentina.
Email: fiorebertone@gmail.com

Funding information
GeoRayos II and CITEDEF with the Proyect GeoRayos II WEB, Grant/Award Number: GINKGO 03 NAC 040/19; Plataforma de Informacion de Riesgo Medioambiental; Ministerio de Defensa, Grant/Award Number: MINDEF PIDDEF 07/18

Abstract

Storms are one of nature's most dangerous phenomena; therefore, knowing their spatial distribution and evolution over time is of great interest for the protection of society, as well as for climate change adaptation strategies. The measurement of Thunderstorm days (Td) was one of the first tools used to monitor storms. The advent of automatic detection networks on the surface has allowed us to advance in the understanding and characterization of the electrical activity in the atmosphere, locating in real-time electrical discharges and providing information over previously unrecorded regions. This work focuses on the integration of human observations at conventional meteorological stations and the data provided by the WWLLN surface discharge detection network in Argentina. The calibration methodology applied determined a mean human thunderstorm detection radius of 21 km which allowed the elaboration of isokeraunic maps for the period 2008–2017 for the region of interest. The spatial distribution of storms yielded the highest values of Td in the Argentine Northwest region with values above 100 Td·year^{-1} followed by a relative maximum in the Argentine Northeast with 80 Td·year^{-1} and the Sierras de Córdoba with 50 Td·year^{-1}.

KEYWORDS

Argentina, lightning, thunder day, thunderstorm

1 | INTRODUCTION

Thunderstorms are undoubtedly one of nature's most amazing meteorological phenomena. The majestic cumulonimbus and the spectacle of light and sound offered by electrical activity (lightning and thunder) have attracted human attention since ancient times. However, thunderstorms are dangerous and damaging meteorological events. In the mid-latitudes, they are among the main causes of weather-related economic losses and human deaths (Holle *et* al., 2000; Sasse and Hauf, 2003; Larjavaara *et al.*, 2005; Mäkelä *et al.*, 2014).

The study of thunderstorms has always presented a difficult challenge due to their large temporal and spatial variability. Initially, human observations from observation stations were the only source of information for climatological studies. Towards the end of the 20th century, with the advent of lightning detection networks, that allowed real-time estimation of thunderstorm location with increasing accuracy, it was possible to advance in the knowledge of the temporal and spatial variability of storms, which up to that moment were biased by several factors (orography, spatial inhomogeneity, relocation of meteorological stations,

population growth, location of nearby airports, among others).

The main climatological variable related to thunderstorm activity is the so-called thunderstorm day (Td). This standard meteorological unit was first defined by the International Meteorological Committee in Vienna in 1873 as a calendar day where thunder is heard at least once, without discriminating whether the discharge is cloud-to-cloud or cloud-to-ground and regardless of the intensity of the thunderstorm or the occurrence of precipitation. Any exceptions to this definition were those days when lightning was observed but no thunder was heard. It is important to note that this definition is strongly dependent on the possibility of hearing thunder. Although Fleagle (1949) in his publication "The Audibility of Thunder" concluded that thunder originating 4 km above the surface on the Earth, can be heard within a radius of approximately 25 km under certain meteorological conditions; in more recent publications, different authors found observation radius ranging between 15 and 25 km (Rakov and Uman, 2007; Mäkelä *et al.*, 2014; Czernecki *et al.*, 2016; Montana *et al.*, 2021).

Given the relevance of the study of thunderstorm activity, Td was introduced as a new Essential Climate Variable in the framework of the GCOS-2016 Implementation Plan (WMO GCOS, 2019). To follow up on this action, the Atmospheric Observations Panel for Climate (AOPC) agreed during AOPC-22 (Exeter, UK, March 2017) to create a dedicated Task-Team on Lightning Observations for Climate Applications ("Task-Team on Lightning Observations for Climate Applications"—TTLOCA).

The first international reference of thunderstorm days in Argentina is in Brooks (1925), where the first study on THE DISTRIBUTION OF THUNDERSTORMS OVER THE GLOBE can be read. The data shown for Argentina were compiled by Davis in his study of the Climate of Argentina in 1902, which shows the long tradition of the country in the study of Td. Later, on September 9, 1952, during the Executive Committee meeting of the World Meteorological Organization (WMO) agreed to prepare global Td tables and maps. Thus, in 1953, Td data were collected from 3,840 meteorological stations in 190 countries around the world, and the document "Distribution of Thunderstorms Days Part I Tables" was prepared. For this document, Argentina shared data from 42 weather stations, as it can be seen in Figure 1. Three years later, in 1956, the WMO published the first global map of Td as part of the document "World Distribution of Thunderstorms Days Part II." These maps coined the term Isokeraunic Maps. The isokeraunic maps show the regions with an equal number of thunderstorm days for a given time period.

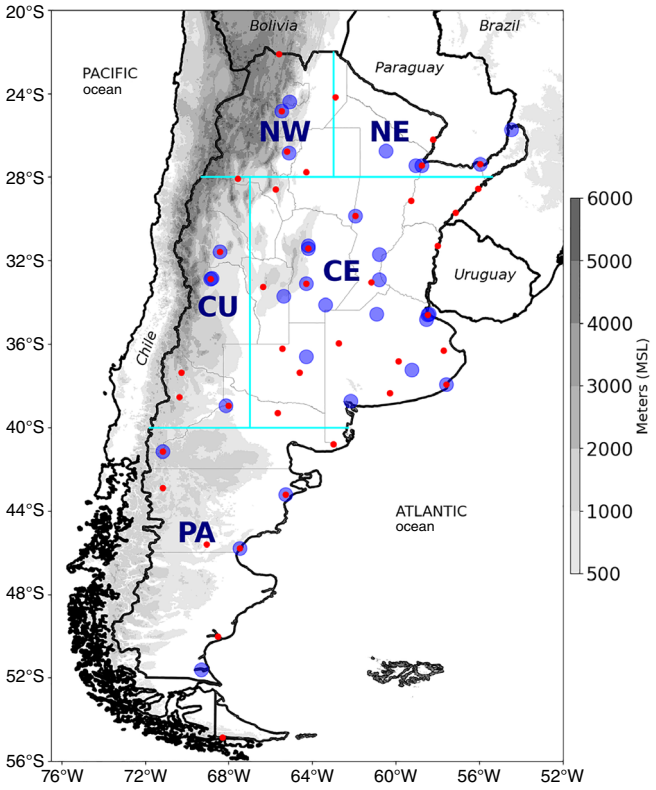

FIGURE 1 Location of the synoptic surface stations used in the study (blue-filled circles) and stations used in the WMO 1956 report (red dots). Different geographical regions also are shown (NO: Northwestern Argentina; NE: Northeastern Argentina; CE: Central Argentina; CU: Western Argentina - Cuyo region; and PA: Patagonia Argentina). Terrain elevation (in meters; grey scale) is from the shuttle radar topography mission

In Argentina, the first isokeraunic maps were elaborated from human observations made by observers of the National Meteorological Service (NMS). Nowadays decadal isokeraunic maps are available from 1960 to 1989 compiled by Hordij *et al.* (1996) and continued by Bordon *et al.* (2009) who re-analysed the decades 1960–1970, 1971–1980, 1981–1990 and incorporated the decade 1991–2000. Those authors conclude that a Td increase is evident in the Patagonian coast and the Paraguay basin. More recently, Arcioni (2006) published in the April 2006 issue of the journal Ingeniería Eléctrica isokeraunic maps for the period 1971–1980 based on the climatological statistics of the NMS. However, given the heterogeneous and insufficient spatial coverage of Argentina's surface synoptic network, maps based on these data alone may not be fully representative of thunderstorm activity (Rasmussen *et al.*, 2014; Albrecht *et al.*, 2016).

In order to elaborate an equivalent map based on data from surface-based lightning detection networks, a Td should be defined as those days in which the network

detects at least one lightning stroke within a given area centred around each station. Several studies have been carried out to find an approximate radius of human detection of thunderstorms using different methods, with the objective of joining the long-term time series and also to find more modern methodologies for its determination. The results show that there is an important dependence on several factors such as orography or time of day in the obtained radius of human detection, with values in the range of approximately 10–26 km (Reeve and Toumi, 1999; Mäkelä *et al*., 2014; Huryn *et al*., 2015; Czernecki *et al*., 2016; Núñez Mora *et al*., 2019).

The main objective of this study is to analyse the relationship between human thunderstorm observations (SYNOP reports) and lightning detection data from the WWLLN network in Argentina for the period 2008–2017. We attempt to define the average human thunderstorm detection range and evaluate thunderstorm measurements over particular weather stations. In addition, the isokeraunic maps obtained will allow us to advance in the knowledge of the climate in Argentina and thus respond to the requirements of TTLOCA in terms of complementing human observations with automatic detection systems.

2 | DATA

2.1 | Synoptic surface network

SYNOP (surface synoptic observations) messages are a numerical code (called FM-12 by the WMO); used to report meteorological observations made by surface weather stations. The current surface network of the NMS of Argentina has 125 stations that perform observations with different work plans prioritizing measurements at 0000, 0600, 1200, and 1800 UTC, known as synoptic hours. In the present work, data from stations that made uninterrupted 24-hr observations during the period 2008–2017 were used (32 stations; Figure 1 and Table 2). Figure 1 also shows the stations presented in the WMO report, in order to provide a historical context regarding the change in the spatial distribution of the stations since the beginning of the 20th century. The difference observed in the location of the blue and red dots in Figure 1 is due to some of the following reasons:

1. Stations used for the elaboration of the 1956 climatology ceased to function before 2007.
2. Stations used for the elaboration of the 1956 climatology were replaced by nearby stations which did not provide uninterrupted 24-hr observations in the period of interest.
3. Similarly, stations used for the elaboration of the 1956 climatology that continue to operate but did not provided uninterrupted 24-hr observations in the period of interest.
4. Stations used for the elaboration of the 1956 climatology that closed and were replaced by nearby stations.

Due to Argentina's varied orography and geographical extension, a large spatial and temporal variability characterizes thunderstorms in Argentina. For this reason, in the present study, the Argentine territory was divided into five regions: Northwest Argentina (NW), Northeast Argentina (NE), Central Argentina (CE), Cuyo (CU) and Patagonia (PA) in order to analyse the particularities present in each one of them (see Section 4.1 below). These regions were defined based on previous studies of deep moist convection (DMC) documented by several authors using satellite data. For more details see Romatschke and Houze (2010), Rasmussen et al. (2011), and Rasmussen *et al*. (2014).

In order to have complete records of Td at each station, we first took into account those days in which the observer reported any of the following present weather codes (hereafter TPres) in the SYNOP message: 13 (lightning without hearing thunder), 17 (Thunderstorm, but no precipitation at the time of observation), 29 (Thunderstorm [with or without precipitation]), 91 (Slight rain at the time of observation), 92 (Moderate or heavy rain at time of observation), 93 (Slight snow, or rain and snow mixed or hail at time of observation), 94 (Moderate or heavy snow, or rain and snow mixed or hail at time of observation), 95 (Thunderstorm, slight or moderate, without hail), 96 (Thunderstorm, slight or moderate, with hail), 97 (Thunderstorm, heavy, without hail but with rain and/or snow at the time of observation), 98 (Thunderstorm combined with dust storm or sandstorm at time of observation), and 99 (Thunderstorm, heavy, with hail at time of observation). In the addition, we take into account the information from the Daily Table (hereafter, TDiar) of the "Hydrometeors and Phenomena" was taken into account in which the observer at the station only notes if at any time during the day they hear any thunder. Both sources of information were subject to rigorous quality control to eliminate erroneous data, evaluate the limitations of the observations, and to prepare an improved Td database. This was carried out by comparing the data from TPres and those provided by TDiar. Different cases emerged from this comparison:

1. Days with thunderstorms were reported in both TPres and TDiar
2. Days with thunderstorms were reported in TPres but not in TDiar

3. Days with thunderstorms reported in TDiar with TPres referring to the hour preceding 0000 hr.
4. Days with thunderstorms were reported in TDiar but not in TPres
5. Days with thunderstorms reported in TDiar with TPres 13 only.
6. Days with TPres 13 and no report in TDiar.

Considering these six cases, it was decided to consider cases 1 and 2 as storm days, and discard case 4 situations because they did not register TPres referring to storms in the SYNOP message. For case 3 situations, since the observation is made at 0000 LST (0300 UTC) but the phenomenon corresponds to the preceding hour (i.e., the previous calendar day), the previous day was considered a storm day, and the day of the TDiar measurement was discarded. For example, in a storm that occurs between 2330 and 2355 LST (0230 and 0255 UTC, respectively) the moment, the phenomenon is recorded, that is, at 0000 LST of the following day, the observer reports the phenomenon with a present time of the preceding hour and in the TDiar of the present day, being that the event occurred the previous day. Case 5 records, which take into account cases where the observer sees lightning but does not hear thunder, were discarded. An example of this case could be given in those stations with a wide field of view in which it is possible to observe storm clouds and see lightning in the distance but not hear thunder. Such cases would add inconsistency between the two datasets because de definition if only lightning is observed, it is incorrect to consider it as a Td. On the contrary, case 6 situations, do not represent any inconsistency between the two datasets because if only lightning is seen (TPres 13) and thunder not heard it should not be reported as a thunderstorm day in the TDiar, therefore it was discarded as Td.

In conclusion, cases 1, 2, and the day before case 3 were considered thunderstorm days, and make up the database used in the elaboration of the isokeraunic maps.

2.2 | WWLLN network

The World Wide Lightning Location Network (WWLLN, http://wwlln.net) is a worldwide network that became operational in August 2004 and has more than 70 stations over different continents. It detects very low-frequency radio waves (spherics) emitted by discharges (Hutchins *et al.*, 2012; Virts *et al.*, 2013). This global network has shown the importance of having a scientific network that covers the entire globe, reaching places where conventional networks do not have coverage; allowing the study of remote locations (Garreaud *et al.*, 2014). This network allows the detection of discharges with an overall accuracy of 10 km and <30 μs (Rodger *et al.*, 2014). The overall efficiency of the WWLLN network in detecting discharges ranges from 5 to 10%, although recent studies estimate that the overall efficiency has reached values around 15% in 2017 (Koronczay *et al.*, 2019). The network calculates daily Relative Detection Efficiency, and as a result of the coverage of stations around the globe, the efficiency in our region of study as calculated in the last few years is between 90 and 100%.

3 | METHODOLOGY

A Td is defined by SYNOP data if at least once a day, the meteorological observer hears thunder at the weather station, and by WWLLN if at least one stroke is detected by the network inside different detection ranges (from 10 to 30 km, with steps of 1 km) centred at the 32 weather stations from the SMN operational 24-hr surface network for the period 2008–2017.

To obtain the range in which humans detect thunderstorms, the methodology proposed by Czernecki *et al.* (2016) was applied. They propose two methods that compare daily Td values from SYNOP messages with those calculated from an automatic detection network (here WWLLN) based on contingency tables.

- **TS method:** compare the SYNOP messages with Td values as calculated using the automatic detection network in an area centred on the meteorological station of interest and considering different radii around it, so that the maximum of the curve obtained (Figure 2) refers to the observation distance that optimizes the Td values of both databases. In addition, the TS value itself estimates the quality of human observations.
- **Delta method:** the Td values reported in the SYNOP messages that were not recorded in the automatic detection network (C in Table 1) are subtracted from the Td values that were reported in the detection network that were not reported in the SYNOP messages (B in Table 1). In this way, the point at which the curve takes the value zero (Figure 2) determines the radius with the best overlap of Td values from both sources of information.

To find the TS and Delta values, a 2 × 2 contingency table (Table 1) is prepared for each detection range and for each of the weather stations, which are calculated as follows:

$$\mathrm{TS} = \frac{A}{A+B+C}.$$

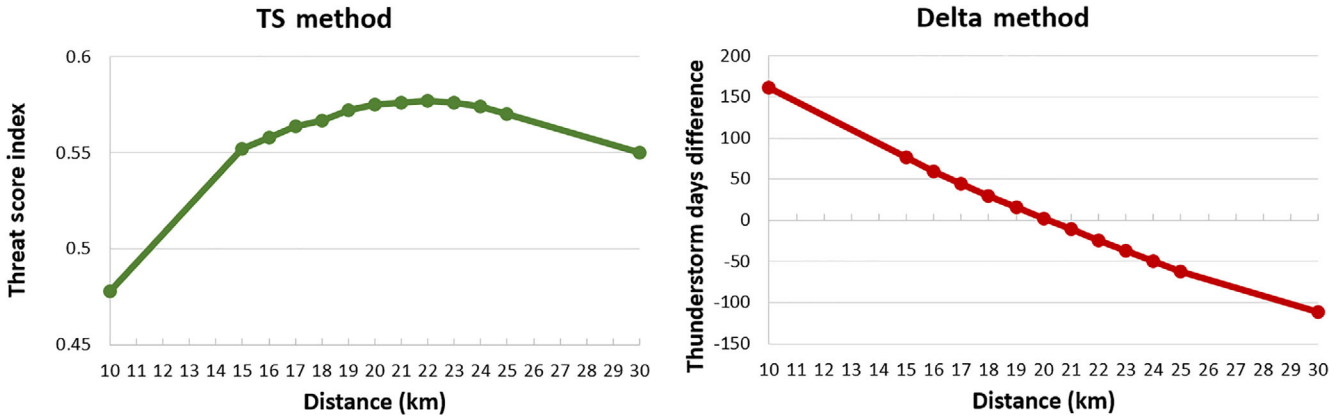

FIGURE 2 (a) TS curve computed as a relationship between lightning detection network data and SYNOP daily thunderstorm reports for certain observational detection range thresholds (radius) within the meteorological station. The highest TS value denotes the threshold with the best observational performance. (b) Delta curve computed as the difference between the number of thunderstorm days derived from the lightning detection network and SYNOP reports for certain observational detection range thresholds (radius) from the meteorological stations. The zero point denotes the threshold with the best observational performance. In both methods, the curves represent the average of the 32 meteorological stations of interest, including data from the period 2008 to 2017

TABLE 1 Number of days with and without storms for a station obtained by SYNOP messages and by a detection network for a particular radius

Thunderstorm reported in SYNOP report	Lightning flash detected by WWLLN network	
	Yes	No
Yes	A	B
No	C	D

$$\text{Delta} = C - B.$$

The above methodology was applied for different radii varying between 15 and 25 km every 1 km and then, to make a more general characterization, every 5 km for distances from 10 to 15 and 25 to 30 km. To compare the Td results obtained for the two datasets, the Student's test for two independent samples was used. The purpose is to test the null hypothesis that states that the difference between the means obtained for two samples zero, that is to say,

$$\overline{\text{Td(WWLLN)}} - \overline{\text{Td(SYNOP)}} = 0.$$

Finally, we use the observational distance values obtained from the TS and Delta methods to calculate, the average annual number of thunderstorm days using WWLLN data heard by humans. To achieve this, we use a uniform grid of $0.05^\circ \times 0.05^\circ$ ($\sim 5 \times 5$ km) bins and at each bin, we take into account flashes within the radius of the obtained threshold value (the average of TS and Delta methods) from the centre of the bin, for the whole 10-year dataset of interest. The seasonal average maps (Figure 6) are calculated in the same way. All calculations mentioned in this section were performed with open-source software in Python software.

4 | RESULTS

4.1 | Human observation range of detection

The TS and Delta curves averaged for the 32 stations are presented in Figure 2. The results show a range of detection of 22 km for TS Method while the Delta method shows a range of detection of 20 km. The mean value of the two methods is 21 km which will be used later in the isokeraunic maps.

These results confirm the estimates of Fleagle (1949) that thunder generated at an altitude of 4 km is rarely heard beyond 25 km, and if generated at lower altitudes, the thunder will be heard within 25 km. Studies of thunder audibility suggest that thunder is heard at distances between 8 and 19 km (Changnon, 1989). Previous work carried out mainly in Europe has found values between 15 and 20 km in southern Germany (Finke and Hauf, 1996), 11.3 km in the Nordic countries (Mäkelä *et al.*, 2014), 17.5 km in Poland (Czernecki *et al.*, 2016), and 10.1 km in Península Ibérica (Núñez Mora *et al.*, 2019).

TABLE 2 Annual and seasonal average number of Td for each station derived from the SYNOP reports and WWLLN network data for the period 2008–2017. These 32 stations are represented by the blue dots in Figure 1

Station	WMO	Latitude (°S)	Longitude (°W)	Altitude (m)	SYNOP					WWLLN				
					Annual	DJF	MAM	JJA	SON	Annual	DJF	MAM	JJA	SON
Aeroparque aero	87,582	34.55	58.41	6	44.9	17.8	8.0	7.4	11.7	47.3	17.6	9.4	8.2	12.1
Bahía Blanca aero	87,750	38.71	62.16	75	40.3	19.3	8.6	1.9	10.5	35.8	17.4	7.2	2.4	8.8
Bariloche aero	87,765	41.14	71.16	835	3.2	2.0	0.7	0.1	0.4	5.9	3.8	1.7	0.1	0.3
Buenos Aires Obs.	87,585	34.59	58.48	25	44.3	17.4	8.1	7.1	11.7	47.2	17.3	9.3	8.5	12.1
Ceres Aero	87,257	29.87	61.93	88	59.0	30.1	10.4	0.9	17.6	53.3	24.1	11.4	2.9	14.9
Comod. Riv. Aero	87,860	45.79	67.46	46	6.0	4.1	1.3	0.0	0.6	4.0	2.6	1.0	0.0	0.4
Córdoba aero	87,344	31.29	64.21	493	52.9	22.5	10.1	3.0	17.3	53.7	28.1	11,0	0.7	13.9
Córdoba Obs.	87,345	31.42	64.19	426	50.2	24.9	9.5	0.5	15.3	52.3	27.7	10.6	0.7	13.3
Corrientes aero	87,166	27.44	58.75	62	75.6	23.8	17.7	9.9	24.2	73.7	24.6	17,0	10,0	22.1
Ezeiza aero	87,576	34.81	58.54	20	43.4	17.4	7.9	6.6	11.5	45.2	17.4	8.6	7.6	11.6
Iguazu Aero	87,097	25.73	54.47	270	82.9	26.1	17.8	13.7	25.3	90.1	31.3	17.6	14.6	26.6
Jujuy aero	87,046	24.38	65.09	921	45.4	29.5	8.6	0.1	7.2	52.9	35.8	8.8	0.3	8,0
Junin Aero	87,548	34.55	60.93	82	53.2	21.3	11.0	4.4	16.5	53.1	21.1	11.9	5.6	14.5
Laboulaye Aero	87,534	34.12	63.36	136	62.0	27.6	12.9	1.9	19.6	54.9	24.6	12.5	2.1	15.7
Mar del Plata Aero	87,692	37.93	57.58	18	38.0	17.5	6.4	4.1	10.0	34,0	16.7	5.2	4.3	7.8
Mendoza Aero	87,418	32.84	68.79	705	35.5	23.4	5.5	0.2	6.4	37,0	24.9	6.3	0.1	5.7
Mendoza Obs.	87,420	32.89	68.87	827	28.7	19.6	4.5	0.1	4.5	38.7	26.4	6.1	0.1	6.1
Neuquen Aero	87,715	38.95	68.13	270	13.5	7.6	2.6	0.0	3.3	14.5	8.2	2.7	0,0	3.6
Pcia. R. S. P. Aero	87,148	26.74	60.48	91	57.3	23.0	13.0	3.5	17.8	58.9	24.3	13.9	3.9	16.8
Posadas Aero	87,178	27.39	55.96	131	77.3	25.9	16.7	12.2	22.5	84.5	29,0	18.2	13.7	23.6
Resistencia Aero	87,155	27.43	59.04	53	78.0	25.7	17.1	10.1	25.1	73,0	26,0	17.1	8.7	21.2
Rio Cuarto Aero	87,453	33.09	64.27	420	64.3	28.9	13.1	1.9	20.4	57.1	28.4	11.3	1.2	16.2
Rio Gallegos Aero	87,925	51.61	69.30	20	4.2	2.6	0.7	0.0	0.9	2.3	1.3	0.5	0.1	0.4
Rosario Aero	87,480	32.90	60.78	25	60.9	23.5	12.0	5.9	19.5	55.7	23,0	11.7	5.4	15.6
Salta Aero	87,047	24.84	65.47	1,221	43.7	31.3	7.1	0.1	5.2	52.6	37.8	9.2	0.1	5.5
San Juan Aero	87,311	31.57	68.42	597	23.2	15.4	3.3	0.0	4.5	28.1	20.2	3.9	0.0	4.0
Santa Rosa Aero	87,623	36.59	64.27	190	51.3	24.7	9.2	1.5	15.9	46.7	23.8	9.3	1.2	12.4
Sauce Viejo Aero	87,371	31.70	60.80	17	53.1	21.4	11.3	4.4	16.0	58.3	23.8	13,0	5.3	16.2
Tandil Aero	87,645	37.24	59.23	175	47.2	20.8	8.6	4.7	13.1	39.8	17.7	8,0	4.3	9.8

(Continues)

TABLE 2 (Continued)

Station	WMO	Latitude (°S)	Longitude (°W)	Altitude (m)	SYNOP				WWLLN					
Trelew aero	87,828	43.20	65.28	39	6.5	4.1	1.4	0.1	0.9	8.9	5.4	1.7	0.0	1.8
Tucuman aero	87,121	26.83	65.10	440	43.1	25.2	7.1	0.1	10.7	51.5	32,0	8.7	0.5	10.3
Va. Reynolds Aero	87,448	33.71	65.37	485	74.9	36.4	14.6	1.2	22.7	59.7	31.4	11.6	0.9	15.8

When comparing the mean annual number of storm days obtained from WWLLN data within a 21 km radius with the mean annual number of storm days derived from SYNOP reports (Table 2), the resulting mean annual value with SYNOP data (WWLLN) is 45.8 (45) days with a 5.8-day mean. If we assume that the results obtained with the WWLLN network represent the true distribution of storm days in Argentina, the resulting percentage error is 13%. This represents the error in the number of annual storm days when only SYNOP data are considered. As expected, this error depends on the time of the year, with a maximum value in spring (22.7%) and a minimum value in autumn (12.4%). During summer, the error amounts to 15% and during winter 19.7%. The scatterplot between the number of annual mean Td from SYNOP observations and WWLLN network data (Figure 3) shows a correlation coefficient of 0.9652.

Although the annual mean values considering all stations are similar, when the differences per year are analysed, they vary between the different stations as shown in Figure 4.

In order to quantify the differences between WWLLN and SYNOP at each of the stations throughout the years of study, the Student's test was applied. The results obtained indicate that out of the 32 stations analysed, in 28 of them the mean differences are not significant at 95%. They are however, significant at Bariloche Aero, Mendoza Observatory, Rio Gallegos Aero and Villa Reynolds Aero, as indicated with a "(*)" in the titles of Figure 4.

When analysing the year-to-year differences in the stations, it is interesting to mention that in most of the stations, between 2008 and 2014, WWLLN underestimated Td. This is consistent with Kaplan and Hong-Kiu Lau (2021), where they point out that in 2014 the WWLLN detection efficiency reached its maximum.

4.2 | Annual isokeraunic map

As mentioned above, Argentina presents a large temporal and spatial variability of thunderstorms, as the spatial distribution of annual thunderstorm days (Figure 5) in different regions of Argentina (Figure 1) will be analysed in order to highlight their individual particularities.

4.2.1 | Northwest region (NO)

This area, which is characterized by a very heterogeneous topography and has mountain peaks of more than 6,000 m above sea level, records the highest values of Td in the whole country, reaching 100 Td·year^{-1}.

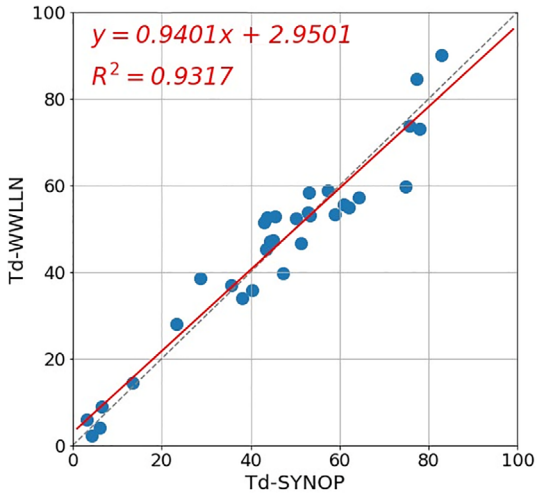

FIGURE 3 Scatterplot of the annual mean number of thunderstorm days from SYNOP versus WWLLN network data for a detection range of 21 km. The red line represents the linear regression model

In addition, a very marked gradient can be observed, especially over the province of Jujuy, with a north–south orientation.

This local maximum respond to the interaction between the Chaco Low and the South American Low-Level Jet (SALLJ) that favour the transport of warm and humid air towards subtropical latitudes, providing favourable conditions for the generation of DMC (Seluchi and Marengo, 2000; Saulo *et al.*, 2004; Ferreira, 2008).

Vidal (2014) also shows this region as one of the most favourable areas in the country for the development of mesoscale convective systems (MCS). According to their study, MCSs in this region are small, stationary and develop in phase with radiative heating in an environment characterized by a high-level anticyclone associated with the Bolivian High, a weak stationary frontal zone, and a northerly flow at low levels with local circulations associated with the Andes mountains. More recently, Ramezani *et al.* (2019) also found that solar heating and high temperatures trigger DMC and extreme rainfall in this region.

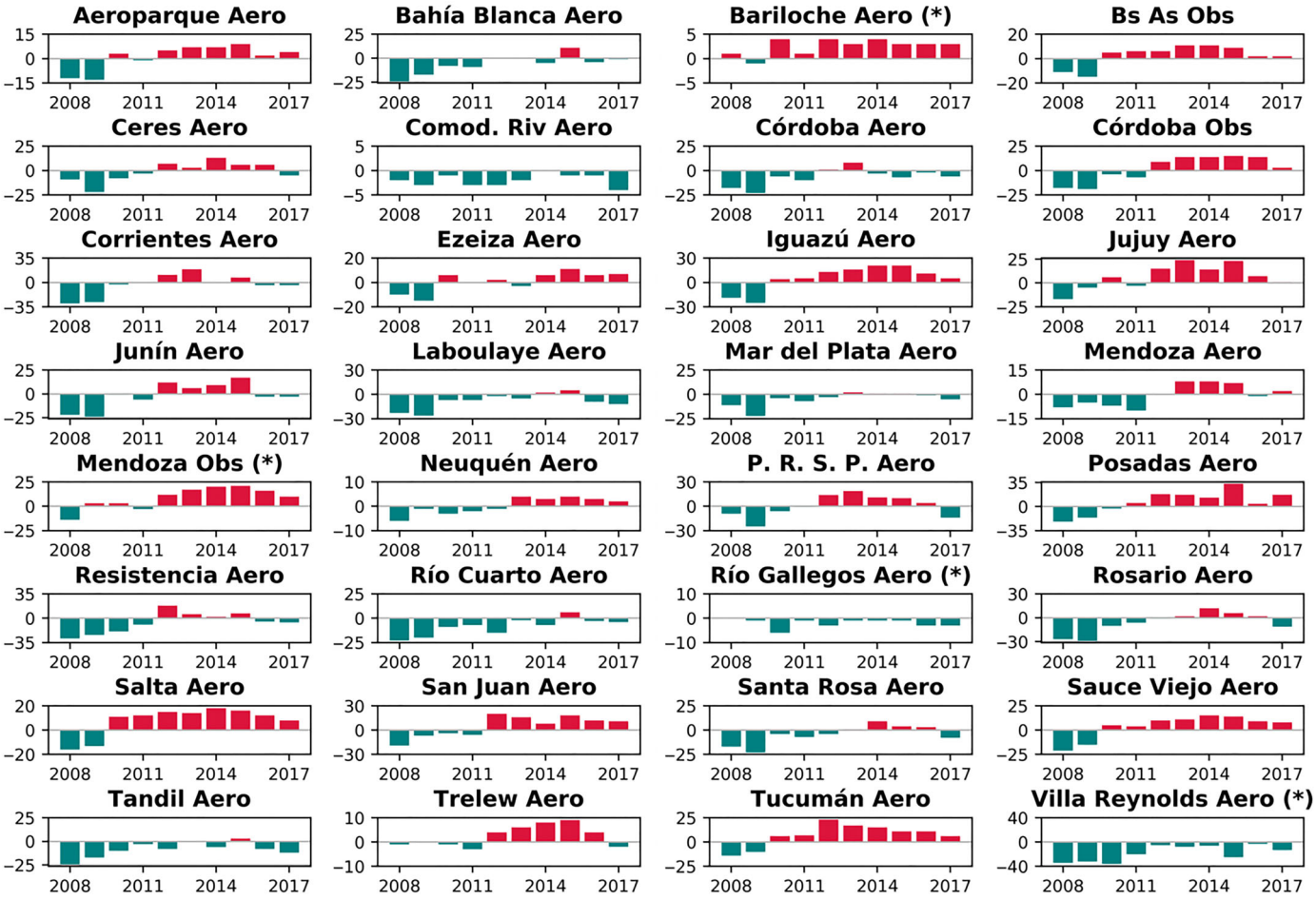

FIGURE 4 Annual differences between the number of thunderstorm days (Td) obtained from WWLLN data within a 21 km radius and the annual number derived from SYNOP reports

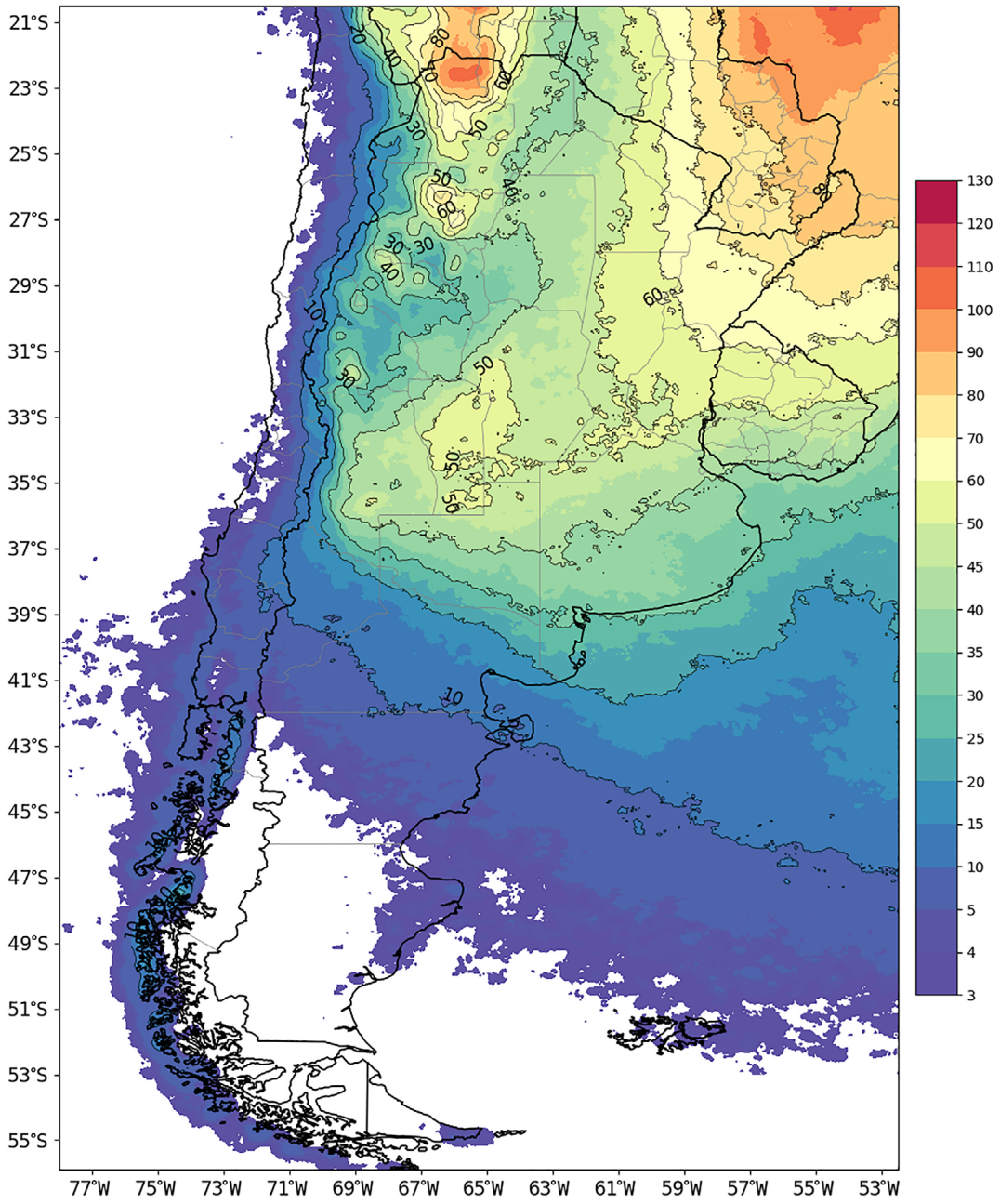

FIGURE 5 Spatial distribution of average annual number of thunderstorm days computed with a threshold on detection range of 21 km and based on the WWLLN lightning detection network data for the period 2008–2017

4.2.2 | Northeast region (NE)

In this area, the annual isokeraunic map shows an increase in Td towards the northeast that reaches values greater than 80 Td·year^{-1} over Misiones. Based on satellite observations, Albrecht *et al.* (2016) identify this region as one of the regions with the highest density of electrical activity in the world, while Bang and Cecil (2019) found the most frequent occurrence of severe storms with hail diameters of 2.5 cm or more, especially in spring and early summer. Matsudo and Salio (2011) after analysing present weather reports of extreme events and satellite observations indicate that extreme rainfall events (>300 mm·day^{-1}) associated with convection have a maximum north of 30°S and east of 62°W associated with the location of extreme MCSs. Anabor *et al.* (2008) studied MCSs in the La Plata River Basin using infrared images from the GOES-12 satellite and information from the NCEP/NCAR reanalysis. They point out that these systems start in the southern region of the La Plata River

Basin in the warm sector of a cyclone near the Atlantic coast with CAPE values above 1,200 $J \cdot kg^{-1}$ and then propagate and dissipate towards the north and northwest of Argentina in conjunction with an anticyclone that crosses the Andes mountain range and would partly explain this northward movement.

The South Atlantic Convergence Zone (SACZ) is another mechanism that affects the occurrence of summer DMC in northern Argentina. This pattern appears as an elongated zone of cloudiness and precipitation that extends diagonally from the northwest to southeast from the Amazon to the South Atlantic. When the SACZ is weak, it induces moisture convergence at low levels and upward movements that favour the development of precipitation in northern Argentina, Paraguay, and southern Brazil (Nogués-Paegle and Mo, 1997; Liebmann *et al.*, 1999; Liebmann *et al.*, 2004; Marengo *et al.*, 2004; Seluchi and Chan Chou, 2009).

4.2.3 | Central region (CE)

Relative Td maximums are found in this region in the Sierras de Córdoba (SCBA) with annual averages greater than 50 $Td \cdot year^{-1}$. Similar results were found by pioneers like Brooks (1925), which showed a maximum frequency of thunderstorms at Córdoba between the late afternoon and early morning of the next day. Most recently, several authors using satellite observations have revealed that this region presents one of the most favourable natural scenarios for the onset of the most intense convective systems in the world with a mostly nocturnal (Zipser *et al.*, 2006; Romatschke and Houze, 2011; Houze *et al.*, 2015). The unique characteristics of this region prompted in November 2018 deployment of the RELAMPAGO-CACTI field experiment (Nesbitt *et al.*, 2021).

Regarding the onset of the DMC originating in this region, several authors suggest that the presence of the SALLJ is a feature closely linked to the conditions preceding the formation of convection (Vera *et al.*, 2006; Salio *et al.*, 2007; Vidal, 2014). In particular, Salio *et al.* (2007) showed in a 3-year analysis that 41% of the subtropical MCSs (south of 23°S) start on SALLJ days, while in the absence of SALLJ this frequency drops to 12%. In relation to this point, Vidal (2014) points out that the characteristics of the synoptic environment favourable for the onset of convection, in addition to the SALLJ, the presence of a frontal zone that favours convergence at low levels and upward movements is necessary.

Liu *et al.* (2010) used TRMM satellite-derived and re-analysis data over a 16-year period to analyse the large-scale favourable environments for the occurrence of intense thunderstorms (>33 lightning strikes per minute). In the case of SCBA, they point out that convection is favoured orographically by warm and moist air supplied by the SALLJ at low levels and by drier and warmer air within the boundary layer due to subsidence on the eastern side of the mountain, while a weak trough is observed at mid-levels (500 hPa) in the lee of the Andes.

DMC in the region originates most frequently at the end of the day and then organizes into large MCSs. These systems develop and extend eastward to then form extensive stratiform precipitation zones that dominate the precipitation climatology on the eastern slope of the SCBA and further east in the plains region. They dissipate later as they are affected by a northward advance of a baroclinic zone related to the horizontal advection of cold air and the divergence of moisture at low levels (Salio *et al.*, 2007; Rasmussen and Houze, 2011; Rasmussen *et al.*, 2014; Mulholland *et al.*, 2018). According to the results of Matsudo and Salio (2011) the NW-SE distribution of these MCSs is associated with the presence and interaction with frontal zones that are more frequent south of 30°S.

Through satellite observations and surface data, several studies that analysed the occurrence of severe weather phenomena associated with these storms, such as hail and tornadoes, coincide in pointing out that hail is very frequent east of the Andes and the SCBA, mainly between spring and summer (Mezher *et al.*, 2012; Rasmussen *et al.*, 2014; Bruick *et al.*, 2019). In particular, Kumjian *et al.* (2020) documented the occurrence of giant hail (diameter greater than 15 cm) associated with a supercell that affected the city of Villa Carlos Paz (Córdoba) in February 2018, very close to the world record in Vivian (South Dakota) with a maximum dimension of 20 cm (Pojorlie *et al.*, 2013).

4.2.4 | Cuyo region (CU)

In this region, which includes the highest peak of the Andes Mountains, the annual isokeraunic map shows a west–east Td gradient and maxima reaching values of 45 $Td \cdot year^{-1}$ in the centre and east of Mendoza. As in the NO and CE regions, the interaction between the topography and the atmosphere generates favourable conditions for the onset and intensification of DMC (de la Torre *et al.*, 2011; Rasmussen and Houze, 2011; Rasmussen *et al.*, 2014). Rosenfeld *et al.* (2006), in a 4-year study (2000–2003) in Mendoza, indicates that in 60% of the days of the warm season (October to March) deep convection is observed, 18% of the days hail is observed, and

in 12% of the days severe hail (diameter >2 cm) is observed. Mezher *et al.* (2012) point out that hail reports are maximized between November and March. These events cause great damage to the agricultural activity and in the region which is why the Anti-Hail Control Program has been in place for many years. de la Torre *et al.* (2011) analysed three severe hailstorms using remote sensing data and numerical model simulations. They also observed mountain waves prior to the onset of these storms and suggest that these waves could be a sufficient mechanism for upward motions leading to convection initiation.

4.2.5 | Patagonia region (PA)

Towards lower latitudes, the isokeraunic map shows an increase in Td values in an SW–NE direction from the centre of Patagonia towards the central plains of the country. The Td values grow in magnitude south of Mendoza where they vary between 20 and 45 Td·year^{-1}. Bechis *et al.* (2019) point out that this region develops adequate conditions for the formation of dry lines. According to the authors, these dry lines define a boundary between air masses characterized by a strong humidity gradient at low levels that favours the development of DMC. In the rest of the Patagonia region, east of the Andes, thunderstorms are less frequent due to the forced subsidence of the eastern side of the Andes, which leads to dry and stable conditions (Garreaud and Gutiérrez, 2001; Garreaud *et al.*, 2014).

4.3 | Seasonal maps

To analyse the seasonal distribution of the thunderstorm days, seasonal maps were computed as shown in Figure 6. The most evident characteristic is a shift of the storm activity towards the northeast from summer to winter with the northeastern region and the east of the province of Buenos Aires being the only regions of the country in which storms occur throughout the year (Figure 6).

The spatial distribution of Td in summer (DJF; Figure 6a) is similar to the annual pattern (Figure 5). Maximums are observed in the NO region with values exceeding 60 days in the north-central Jujuy, and 50 days on the border between Catamarca and Tucumán. There are also relative maximums in the NE region with values exceeding 25 days (Misiones and the east of Formosa). In central Argentina (SCBA, San Luis, and eastern Mendoza) the average value is 30 days. As mentioned above, it is in central Argentina where subtropical MCSs are most frequent during summer (Salio *et al.*, 2007; Romatschke and Houze, 2010; Matsudo and Salio, 2011; Rasmussen and Houze, 2011; Vidal, 2014; Mulholland *et al.*, 2018; Liu *et al.*, 2020). According to the SALLJ event classification proposed by Nicolini and Saulo (2006), Chaco Jet events occur when maximum wind reaches latitudes south of 25°S and occur 17% of summer days, explaining part of the convective activity in central and eastern Argentina (Salio *et al.*, 2002; Nicolini and Saulo, 2006; Salio *et al.*, 2007).

Rasmussen and Houze (2011), using 11 years of TRMM satellite data, found that storms with broad convective cores are the most frequent in the NO and CE regions with a seasonal maximum between December and January, while storms with deep convective cores are more numerous in the SCBA and the southern region of the La Plata Basin. Rasmussen *et al.* (2014) locate a nocturnal maximum of electrical activity in central Argentina near the SCBA and the eastern Andes, and Cecil (2009) indicates that 60% of the storms with at least 125 discharges per minute report hail.

At higher latitudes, in northern Patagonia (Figure 6a), a Td gradient is observed with values between 10 and 25 Td·year^{-1}, although it is less marked than in the annual map. In this region, Bechis *et al.* (2019) indicate that it is towards the end of spring and summer when the highest frequency of dry lines occurs, with increasing frequency towards western Patagonia.

Autumn (MAM) is a transition season in which the SALLJ becomes weaker and the influence of the intensification of the South Atlantic anticyclone that brings moisture to the continent. The maximum Td remains as in the summer located over Jujuy with a strong decrease, now barely exceeding 20 Td·year^{-1}, while in the NE and the SCBA values of 15 and 10 Td·year^{-1} are observed, respectively. Possia (2004) points out the Argentinean coast as a region where explosive cyclogenesis is most frequent in the country. The extraordinarily rapid development of these systems is responsible for phenomena such as intense winds, heavy rains, and electrical activity in the region.

In winter (JJA), when the passage of cold fronts is more frequent, there is a clear eastward displacement of thunderstorm activity. A zonal gradient is observed in a west–east direction and the maximum Td values cover almost entirely the province of Misiones province with values higher than 10 Td·year^{-1} and with maxima that reaches 15 Td·year^{-1}. During this season, rainfall in eastern Argentina is favoured by the penetration of cold fronts in lower latitudes, intensifying baroclinic conditions that favour the onset and development of DMC (Seluchi and Marengo, 2000).

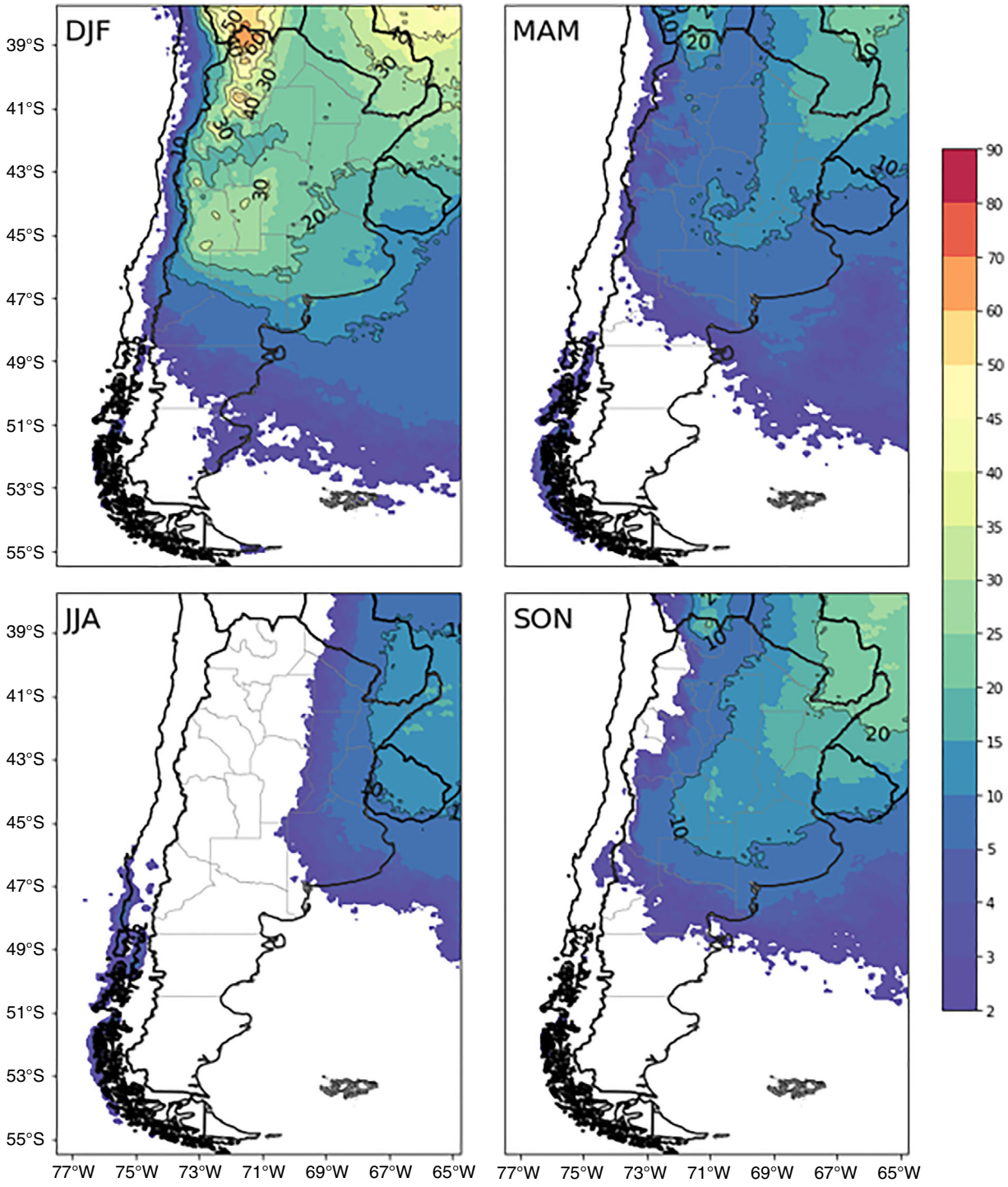

FIGURE 6 Spatial distribution of the seasonal average of the number of thunderstorm days (Td) based on the WWLLN lightning detection network data and assuming a range of detection of 21 km. (a) Summer (DJF), (b) autumn (MAM), (c) winter (JJA), and (d) spring (SON)

In spring (SON), maximum values greater than 20 Td·year^{-1} are observed in the NE region. These results coincide with those obtained by Rasmussen *et al.* (2014) which indicate peak springtime electrical activity in this region associated with thunderstorms with deep or broad convective cores or both, while Cecil and Blankenship (2012) locate in this season the maximum frequency of hail in Paraguay and in the NEA as, estimated from satellite data. Rasmussen and Houze (2011) identified the maximum of thunderstorm days in October in the southern region of the La Plata basin.

5 | CONCLUSIONS

This study presents of the spatial distribution of thunderstorm days in Argentina as calculated from discrete data, we used discrete data from 32 weather stations belonging to the surface synoptic network of the NMS of Argentina and continuous information observed by the WWLLN detection network. We define a thunderstorm day as a day when an observer hears thunder at least once. For the WWLLN network, we define a thunderstorm day when the network detects at least one electrical discharge during the day in a given area centred on the station.

One of the main challenges was to achieve a good integration of these two sources of information. For this purpose, it was necessary to work on the preparation of a robust SYNOP database based on the application of quality controls. These focused on the analysis of present weather reports (codes 13, 17, 29, and 91 to 99) and the Daily Table of the "Hydrometeors and Phenomena" meteorological notebook. Applying quality control allowed, in addition to eliminating erroneous data, to know the limitations of human observations and their documentation in the meteorological notebook.

By using two different methods as proposed by Czernecki *et al*. (2016) (Delta and TS) we defined the average detection range in which humans detect thunderstorms in Argentina, and with the use of data from the WWLLN network, climatological maps of thunderstorm days were prepared according to the way in which lightning would be perceived by humans. One of the main advantages of integrating these data sources and obtaining a human detection range is that it makes it possible to create isokeraunic maps with data calculated by a lightning detection network. This represents a great advance in the study of storm climatology since it allows us to establish and for the first time in some areas, the most frequent areas for discharges, which until now were only established from human records only. A isokeraunic map, made only from discrete SYNOP data, would probably have introduced errors when making interpolations, since the number and spatial distribution of weather stations, at least in the region of interest, is not sufficient to achieve a good representativeness in accordance with the spatial and temporal scale of the storms.

The mean human detection range found was 20 (22) km for the TS (Delta) method resulting in an overall mean value of 21 km. This value may be the most reliable estimate for how humans to perceive thunderstorms in Argentina. The main advantage of the TS method is related to the fact that it also analyses situations where thunderstorms were observed in the SYNOP observations but did not occur in the WWLLN data and vice versa. In contrast, the Delta method does not include such situations and only takes into account the relative sum of Tds derived from the SYNOP and WWLLN datasets.

This study is one of the first in the region, as well as Montana *et al*. (2021) in the Chilean region, to provide such an analysis using such a large database (10 years). Up to now, the only map elaborated in the country using data from a lightning detection network was done by Nicora (2014) for the 2005–2011 period, although the latter was at a lower resolution.

The annual map of Tds shows an absolute maximum located in northwestern Argentina with values greater than 100 Td·year^{-1}, followed by a relative maxima in the northeast (80 Td·year^{-1}) and the SCBA (50 Td·year^{-1}). A similar distribution was observed in the isokeraunic map corresponding to the summer, while in the other seasons a general shift of the electrical activity towards the northeast was observed. It was also shown that in central and eastern Argentina it is possible to observe thunderstorms throughout the year.

However, it is important to mention that some significant differences in the detection radius at some of the stations in our study (e.g., Rio Gallegos, 35 km; Bariloche, 11 km) were found, and this could have an impact on the calculation of Td at each station. It is difficult to explain these differences and an answer can be very complex. As mentioned in the Section 1, each weather station has different location characteristics and weather observers may be more attentive at one than another. In addition, problems of inhomogeneity may be due to the fact that, at some stations, more distant thunder can be heard, while at others, high noise levels or other site-specific factors may reduce the observer's ability to report a thunderstorms (Changnon, 1989). Topography, fast-growing cities that are built over older stations, and station relocations can also influence storm reports. As suggested Reap and Orville (1990), the storm detection range can also be increased at night when there is more silence by adding a few additional kilometres to the detection range (up to 26 km).

Finally, this methodology of integrating human and automatic observations will make it possible to provide continuity (because thunder day observations are continuing today) to the time series at particular weather stations and hence investigate the presence of trends in storm frequency in a climate change scenario. In this way, this information will be of great use in the development of strategic plans that guarantee people's safety and in the planning of adaptation policies in the face of future scenarios, as those presented in Lavigne et al. (2019) on trends in Td and flash density.

ACKNOWLEDGEMENTS

We would like to thank the NMS of Argentina for providing SYNOP data, and the World Wide Lightning Location Network (http://wwlln.net) for providing the lightning location data used in this paper. This research was supported by the Ministerio de Defensa through MINDEF PIDDEF 07/18: Plataforma de Informacion de Riesgo Medioambiental; and GeoRayos II and CITEDEF with the Proyect GeoRayos II WEB and GINKGO 03 NAC 040/19.

ORCID

Fiorela Bertone https://orcid.org/0000-0002-7181-9713
Gabriela Nicora https://orcid.org/0000-0001-7504-6423
Luciano Vidal https://orcid.org/0000-0001-6715-2648

REFERENCES

Albrecht, R.I., Goodman, S.J., Buechler, D.E., Blakeslee, R.J. and Christian, H.J. (2016) Where are the lightning hotspots on Earth? *Bulletin of the American Meteorological Society*, 97(11), 2051–2068. https://doi.org/10.1175/bams-d-14-00193.1.

Anabor, V., Stensrud, D.J. and de Moraes, O.L.L. (2008) Serial upstream-propagating mesoscale convective system events over southeastern South America. *Monthly Weather Review*, 136(8), 3087–3105. https://doi.org/10.1175/2007mwr2334.1.

Arcioni, J.C. (2006) La Actividad Eléctrica Atmosférica Media Anual ('AEAMA') En La Argentina. *Ingeniería Eléctrica*, 130–139.

Bang, S.D. and Cecil, D.J. (2019) Constructing a multifrequency passive microwave hail retrieval and climatology in the GPM domain. *Journal of Applied Meteorology and Climatology*, 58(9), 1889–1904. https://doi.org/10.1175/jamc-d-19-0042.1.

Bechis, H., Salio, P. and Ruiz, J.J. (2019) Drylines in Argentina: synoptic climatology and processes leading to their genesis. *Monthly Weather Review*, 148(1), 111–129. https://doi.org/10.1175/mwr-d-19-0050.1.

Bordon, S., Garrido, R. and Iserte, M.P. (2009) *Curvas De Nivel Isoceráunico En La República Argentina*. X Congreso Argentino De Meteorología (CONGREMET X) y XIII Congreso Latinoamericano e Ibérico De Meteorología (CLIMET XIII).

Brooks, C.E.P. (1925) The distribution of thunderstorms over the globe. *Geophysical Memoirs*, 24, 156-161.

Bruick, Z.S., Rasmussen, K.L. and Cecil, D.J. (2019) Subtropical south American hailstorm characteristics and environments. *Monthly Weather Review*, 147(12), 4289–4304. https://doi.org/10.1175/mwr-d-19-0011.1.

Cecil, D.J. (2009) Passive microwave brightness temperatures as proxies for hailstorms. *Journal of Applied Meteorology and Climatology*, 48(6), 1281–1286. https://doi.org/10.1175/2009jamc2125.1.

Cecil, D.J. and Blankenship, C.B. (2012) Toward a global climatology of severe hailstorms as estimated by satellite passive microwave imagers. *Journal of Climate*, 25(2), 687–703. https://doi.org/10.1175/jcli-d-11-00130.1.

Changnon, S.A. (1989) Relations of thunderstorms and cloud-to-ground lightning frequencies. *Journal of Climate*, 2(8), 897–921. https://doi.org/10.1175/1520-0442(1989)002<0897:rotact>2.0.co;2.

Czernecki, B., Taszarek, M., Kolendowicz, L. and Konarski, J. (2016) Relationship between human observations of thunderstorms and the PERUN lightning detection network in Poland. *Atmospheric Research*, 167(January), 118–128. https://doi.org/10.1016/j.atmosres.2015.08.003.

de la Torre, A., Hierro, R., Llamedo, P., Rolla, A. and Alexander, P. (2011) Severe hailstorms near southern Andes in the presence of mountain waves. *Atmospheric Research*, 101(1–2), 112–123. https://doi.org/10.1016/j.atmosres.2011.01.015.

Ferreira, L. J. (2008) *Causas y variabilidad de la depresión del noroeste Argentino e impactos sobre los patrones regionales de circulación*. PhD thesis, Universidad de Buenos Aires.

Finke, U. and Hauf, T. (1996) The characteristics of lightning occurrence in southern Germany. *Contributions to Atmospheric Physics*, 69, 361-374. https://www.semanticscholar.org/paper/The-Characteristics-of-Lightning-Occurrence-in-Finke-Hauf/54a3f69b75bbace00d485f32ff55d6d07c2baae3.

Fleagle, R.G. (1949) The audibility of thunder. *The Journal of the Acoustical Society of America*, 21(4), 411–412. https://doi.org/10.1121/1.1906528.

Garreaud, R.D., Nicora, M.G., Bürgesser, R.E. and Ávila, E.E. (2014) Lightning in Western Patagonia. *Journal of Geophysical Research: Atmospheres*, 119(8), 4471–4485. https://doi.org/10.1002/2013jd021160.

Garreaud, R. and Gutiérrez, P.A. (2001) Interannual rainfall variability over the South American Altiplano. *Journal of Climate*, 14(12), 2779–2789.

Holle, R.L., Curran, E.B. and López, R.E. (2000) Lightning casualties and damages in the United States from 1959 to 1994. *Journal of Climate*, 13, 3448–3464. https://doi.org/10.1175/1520-0442(2000)013⟨3448:LCADIT⟩2.0.CO;2.

Hordij, H., Bordón, S. and Sassone, R. (1996) *Análisis De La Marcha Anual De Las Cartas Isoceráunicas Mensuales En La República Argentina*. Buenos Aires, Argentina: VII Congreso Argentino De Meteorología y VII Congreso Latinoamericano e Ibérico De Meteorología.

Houze, R.A., Rasmussen, K.L., Zuluaga, M.D. and Brodzik, S.R. (2015) The variable nature of convection in the tropics and subtropics: A legacy of 16Years of the tropical rainfall measuring mission satellite. *Reviews of Geophysics*, 53(3), 994–1021. https://doi.org/10.1002/2015rg000488.

Huryn, S., Gough, W., Butler, K. and Mohsin, T. (2015) An evaluation of thunderstorm observations in Southern Ontario using automated lightning detection data. *Journal of Applied Meteorology and Climatology*, 54(9), 1837–1846. https://doi.org/10.1175/jamc-d-15-0089.1.

Hutchins, M.L., Holzworth, R.H., Rodger, C.J. and Brundell, J.B. (2012) Far-field power of lightning strokes as measured by the world wide lightning location network. *Journal of Atmospheric and Oceanic Technology*, 29(8), 1102–1110. https://doi.org/10.1175/jtech-d-11-00174.1.

Kaplan, J.O. and Hong-Kiu Lau, K. (2021) The WGLC global gridded lightning climatology and timeseries. *Earth System Science Data*, 13, 3219–3237. https://doi.org/10.5194/essd-2021-89.

Koronczay, D., Lichtenberger, J., Clilverd, M.A., Rodger, C.J., Lotz, S.I., Sannikov, D.V., Cherneva, N.V., Raita, T., Darrouzet, F., Ranvier, S. and Moore, R.C. (2019) The source regions of whistlers. *Journal of Geophysical Research:*

Space Physics, 124(7), 5082–5096. https://doi.org/10.1029/2019ja026559.

Kumjian, M.R., Gutierrez, R., Soderholm, J.S., Nesbitt, S.W., Maldonado, P., Luna, L.M., Marquis, J., Bowley, K.A., Imaz, M. A. and Salio, P. (2020) Gargantuan hail in Argentina. *Bulletin of the American Meteorological Society*, 101(8), E1241–E1258. https://doi.org/10.1175/bams-d-19-0012.1.

Larjavaara, M., Kuuluvainen, T. and Rita, H. (2005) Spatial distribution of lightning-ignited Forest fires in Finland. *Forest Ecology and Management*, 208(1–3), 177–188. https://doi.org/10.1016/j.foreco.2004.12.005.

Lavigne, T., Liu, C. and y Liu, N. (2019) How does the trend in thunder-days relate to the variation of lightning flash density? *Journal of Geophysical Research: Atmospheres*, 124, 4955–4974. https://doi.org/10.1029/2018jd029920.

Liebmann, B., Kiladis, G.N., Marengo, J.A., Ambrizzi, T. and Glick, J.D. (1999) Submonthly convective variability over South America and the South Atlantic convergence zone. *Journal of Climate*, 12(7), 1877–1891.

Liebmann, B., Vera, C.S., Carvalho, L.M.V., Camilloni, I.A., Hoerling, M.P., Allured, D., Barros, V.R., Báez, J. and Bidegain, M. (2004) An observed trend in central south American precipitation. *Journal of Climate*, 17(22), 4357–4367. https://doi.org/10.1175/3205.1.

Liu, C., Williams, E.R., Zipser, E.J. and Burns, G. (2010) Diurnal variations of global thunderstorms and electrified shower clouds and their contribution to the global electrical circuit. *Journal of the Atmospheric Sciences*, 67(2), 309–323. https://doi.org/10.1175/2009jas3248.1.

Liu, N., Liu, C., Chen, B. and Zipser, E. (2020) What are the favorable large-scale environments for the highest-flash-rate thunderstorms on Earth? *Journal of the Atmospheric Sciences*, 77(5), 1583–1612. https://doi.org/10.1175/jas-d-19-0235.1.

Mäkelä, A., Enno, S. and Haapalainen, J. (2014) Nordic lightning information system: thunderstorm climate of northern Europe for the period 2002-2011. *Atmospheric Research*, 139(March), 46–61. https://doi.org/10.1016/j.atmosres.2014.01.008.

Marengo, J.A., Soares, W.R., Saulo, C. and Nicolini, M. (2004) Climatology of the low-level jet east of the Andes as derived from the NCEP NCAR Reanalyses: characteristics and temporal variability. *Journal of Climate*, 17, 2261–2280.

Matsudo, C.M. and Salio, P. (2011) Severe weather reports and proximity to deep convection over Northern Argentina. *Atmospheric Research*, 100(4), 523–537. https://doi.org/10.1016/j.atmosres.2010.11.004.

Mezher, R.N., Doyle, M. and Barros, V. (2012) Climatology of hail in Argentina. *Atmospheric Research*, 114-115(October), 70–82. https://doi.org/10.1016/j.atmosres.2012.05.020.

Montana, J., Schurch, R., Nicora, M.G., Aranguren, D., Morales, C. and Ardila-Rey, J. (2021) Lightning activity over Chilean territory. *Journal of Geophysical Research Atmospheres*, 126, e2021JD034580. https://doi.org/10.1029/2021JD034580.

Mulholland, J.P., Nesbitt, S.W., Trapp, R.J., Rasmussen, K.L. and Salio, P.V. (2018) Convective storm life cycle and environments near the Sierras De CóRdoba Argentina. *Monthly Weather Review*, 146(8), 2541–2557. https://doi.org/10.1175/mwr-d-18-0081.1.

Nesbitt, S.W., Salio, P.V., Ávila, E., Bitzer, P., Lawrence Carey, V., Chandrasekar, W.D., et al. (2021) A storm safari in subtropical South America: Proyecto RELAMPAGO. *Bulletin of the American Meteorological Society*, 102, E1621–E1664. https://doi.org/10.1175/bams-d-20-0029.1.

Nicolini, M. and Saulo, A.C. (2006) Modeled Chaco low-level jets and related precipitation patterns during the 1997-1998 warm season. *Meteorology and Atmospheric Physics*, 94(1–4), 129–143. https://doi.org/10.1007/s00703-006-0186-7.

Nicora, M. G. (2014) *Actividad EléCtrica AtmosféRica En SudaméRica*. PhD thesis, Universidad Nacional de La Plata. https://doi.org/10.35537/10915/42231.

Nogués-Paegle, J. and Mo, K. (1997) Alternating wet and dry conditions over South America during summer. *Monthly Weather Review*, 125(2), 279–291. https://doi.org/10.1175/1520-0493(1997)125⟨0279:AWADCO⟩2.0.CO;2.

Núñez Mora, J.A., Riesco Martín, J. and Mora García, M.A. (2019) Climatología De descargas eléctricas y de días de tormenta En España. *Agencia Estatal de Meteorología*, 129-132. https://doi.org/10.31978/639-19-007-7.

Pojorlie, K.L., Doering, S. and Fowle, M. (2013) The record-breaking Vivian, South Dakota, hailstorm of 23 July 2010. *Journal of Operational Meteorology*, 1, 3–18.

Possia, N. (2004) *Estudio De Los Ciclones Explosivos Sobre La Región Sur De Sudamérica*". PhD thesis. https://bibliotecadigital.exactas.uba.ar/collection/tesis/document/tesis_n3786_Possi

Rakov, V.A. and Uman, M.A. (2007) *Lightning: Physics and Effects*. Cambridge, England: Cambridge University Press.

Ramezani Ziarani, M., Bookhagen, B., Schmidt, T., Wickert, J., de la Torre, A. and Hierro, R. (2019) Using convective available potential energy (CAPE) and dew-point temperature to characterize rainfall-extreme events in the South-Central Andes. *Atmosphere*, 10(7), 379. https://doi.org/10.3390/atmos10070379.

Rasmussen, K.L. and Houze, R.A. (2011) Orogenic convection in subtropical South America as seen by the TRMM satellite. *Monthly Weather Review*, 139(8), 2399–2420. https://doi.org/10.1175/mwr-d-10-05006.1.

Rasmussen, K.L., Zuluaga, M.D. and Houze, R.A. (2014) Severe convection and lightning in subtropical South America. *Geophysical Research Letters*, 41(20), 7359–7366. https://doi.org/10.1002/2014gl061767.

Reap, R.M. and Orville, R.E. (1990) The relationships between network lightning surface and hourly observations of thunderstorms. *Monthly Weather Review*, 118(1), 94–108. https://doi.org/10.1175/1520-0493(1990)118<0094:trbnls>2.0.co;2.

Reeve, N. and Toumi, R. (1999) Lightning activity as an indicator of climate change. *Quarterly Journal of the Royal Meteorological Society*, 125(555), 893–903. https://doi.org/10.1002/qj.49712555507.

Rodger, C. J., Brundell, J. B., Hutchins, M. and Holzworth, R. H. (2014) The world wide lightning location network (WWLLN): Update of status and applications. *Proceedings of the 2014 XXXIth URSI General Assembly and Scientific Symposium (URSI GASS)*. IEEE. https://doi.org/10.1109/ursigass.2014.6929581.

Romatschke, U. and Houze, R.A. (2010) Extreme summer convection in South America. *Journal of Climate*, 23(14), 3761–3791. https://doi.org/10.1175/2010jcli3465.1.

Romatschke, U. and Houze, R.A. (2011) Characteristics of precipitating convective Systems in the South Asian Monsoon. *Journal of Hydrometeorology*, 12(1), 3–26. https://doi.org/10.1175/2010jhm1289.1.

Rosenfeld, D., Woodley, W.L., Krauss, T.W. and Makitov, V. (2006) Aircraft microphysical documentation from cloud base to anvils of hailstorm feeder clouds in Argentina. *Journal of Applied Meteorology and Climatology*, 45(9), 1261–1281. https://doi.org/10.1175/jam2403.1.

Salio, P., Nicolini, M. and aulo, A.C. (2002) Chaco low-level jet events characterization during the austral summer season. *Journal of Geophysical Research*, 107(D24), 4816. https://doi.org/10.1029/2001jd001315.

Salio, P., Nicolini, M. and Zipser, E.J. (2007) Mesoscale convective systems over southeastern South America and their relationship with the south American low-level jet. *Monthly Weather Review*, 135(4), 1290–1309. https://doi.org/10.1175/mwr3305.1.

Sasse, M. and Hauf, T. (2003) A study of thunderstorm-induced delays at Frankfurt airport Germany. *Meteorological Applications*, 10(1), 21–30. https://doi.org/10.1017/s1350482703005036.

Saulo, A.C., Seluchi, M.E. and Nicolini, M. (2004) A case study of a Chaco low-level jet event. *Monthly Weather Review*, 132(11), 2669–2683. https://doi.org/10.1175/mwr2815.1.

Seluchi, M.E. and Chan Chou, S. (2009) Synoptic patterns associated with landslide events in the Serra do mar Brazil. *Theoretical and Applied Climatology*, 98(1–2), 67–77. https://doi.org/10.1007/s00704-008-0101-x.

Seluchi, M.E. and Marengo, J.A. (2000) Tropical–midlatitude exchange of air masses during summer and winter in South America: climatic aspects and examples of intense events. *International Journal of Climatology*, 20, 1167–1190. https://doi.org/10.1002/1097-0088(200008)20:10<1167::AID-JOC526>3.0.CO;2-T.

Vera, C., Baez, J., Douglas, M., Emmanuel, C.B., Marengo, J., Meitin, J., Nicolini, M., Nogues-Paegle, J., Paegle, J., Penalba, O., Salio, P., Saulo, C., Silva Dias, M.A., Dias, P.S. and Zipser, E. (2006) The south American low-level jet experiment. *Bulletin of the American Meteorological Society*, 87(1), 63–78. https://doi.org/10.1175/bams-87-1-63.

Vidal, L. (2014) Convección *Extrema Sobre Sudamérica: Estructura Interna, Ciclos De Vida e Influencia De La Topografia En La Iniciación*. PhD thesis, Universidad de Buenos Aires.

Virts, K.S., Wallace, J.M., Hutchins, M.L. and Holzworth, R.H. (2013) Highlights of a new ground-based hourly global lightning climatology. *Bulletin of the American Meteorological Society*, 94(9), 1381–1391. https://doi.org/10.1175/bams-d-12-00082.1.

Zipser, E.J., Cecil, D.J., Liu, C., Nesbitt, S.W. and Yorty, D.P. (2006) Where are the most intense thunderstorms on earth? *Bulletin of the American Meteorological Society*, 87(8), 1057–1072. https://doi.org/10.1175/bams-87-8-1057.

How to cite this article: Bertone, F., Nicora, G., & Vidal, L. (2022). Thunderstorm days over Argentina: Integration between human observations of thunder and the world wide lightning location network lightning data. *International Journal of Climatology*, *42*(16), 9072–9087. https://doi.org/10.1002/joc.7800